Applied Catalysis B: Environmental 168-169 (2015) 490–496

Contents lists available at ScienceDirect

Applied Catalysis B: Environmental

journal homepage: www.elsevier.com/locate/apcatb

Photocatalytic NO removal on BiOI surface: The change from nonselective oxidation to selective oxidation

Guohui Dong[a,c], Wingkei Ho[a,b,*], Lizhi Zhang[c]

[a] Department of Science and Environmental Studies and Centre for Education in Environmental Sustainability, The Hong Kong Institute of Education, Tai Po, N.T. Hong Kong, PR China
[b] Institute of Earth Environment, Chinese Academy of Sciences, PR China
[c] Key Laboratory of Pesticide and Chemical Biology of Ministry of Education, College of Chemistry, Central China Normal University, Wuhan 430079, PR China

ARTICLE INFO

Article history:
Received 25 November 2014
Received in revised form 8 January 2015
Accepted 13 January 2015
Available online 24 January 2015

ABSTRACT

Numerous publications have investigated nitric oxide (NO) removal through semiconductor photocatalytic technology. However, few reports are available on the products and mechanisms of the photocatalytic NO removal process. In this study, BiOI hollow microspheres are synthesized for the photocatalytic removal of NO under the visible light irradiation. Results show that NO removal product and NO removal mechanism could interfere with each other. NO removal process could be changed from nonselective oxidation to selective oxidation as the irradiation time increases. Meanwhile, the product of NO removal could be changed from nitrate (NO_3^-) to nitrogen dioxide (NO_2). These interesting changes were attributed to the generated NO_3^-, which was produced from the reactions between NO and $^{\bullet}OH$. The generated NO_3^- could inhibit $^{\bullet}OH$ generation, thus leading to a change in the NO removal products and NO removal mechanism. This study can improve our understanding of NO removal on the photocatalyst surface and serve as a guide in using photocatalysts for NO removal.

1. Introduction

Nitric oxide (NO) is commonly formed from the combustion of fossil fuel, which supplies energy in the daily lives of people [1]. It is also produced naturally during the electrical discharges of lightning in thunderstorms [2]. NO is considered a common gaseous pollutant because it can cause environmental and health problems, such as acid rain, photochemical smog, haze, and even pulmonary edema [3–6]. NO concentration in the atmosphere has greatly increased over the past few decades because of the increased number of automobiles and industrial activities [7]. Therefore, developing efficient and economical technologies to eliminate NO contamination is necessary. Conventional NO removal methods include physical adsorption, biofiltration, thermal catalysis reduction, acid absorption and alkaline absorption [8–12]. Most of these methods are expensive, complex, and less efficient and may produce secondary pollution. Semiconductor photocatalytic technology has recently been regarded as an attractive alternative technology for NO removal [13,14]. In the photocatalytic process, the photogenerated electrons and holes migrate to the surface of photocatalyst and initiate the generation of reactive species, such as the photogenerated electron (e^-), hole (h^+), superoxide ($^{\bullet}O_2^-$) and hydroxyl radical ($^{\bullet}OH$) [15,16]. Through the redox reaction by these reactive species, NO could be removed effectively [17,18]. Many studies have investigated NO removal through semiconductor photocatalytic technology, but mostly focused on the activity of photocatalysts and the decrease of NO concentration [19–22]. Only few reports focus on the final or by-products of NO removal process. NO can be generally oxidized to different kinds of products, such as NO_2, HNO_2, and HNO_3. However, some of these products such as HNO_3, which can occupy the surface active sites of photocatalyst may have negative effect on the photocatalyst's activity for the removal of NO. Thus, HNO_3 should be washed away or removed from the photocatalyst surface for real application. Investigations on NO removal products can serve as a guide for the proper use of photocatalysts for better NO removal efficiency. Therefore, elucidating the NO removal products and the mechanism involved is essential.

The mechanisms of NO removal remain unclear in literature. NO can be oxidized by either photogenerated hole or other active

* Corresponding author at: Department of Science and Environmental Studies and Centre for Education in Environmental Sustainability, The Hong Kong Institute of Education, Tai Po, N.T. Hong Kong, PR China. Tel.: +85 229488255.
E-mail address: keithho@ied.edu.hk (W. Ho).

http://dx.doi.org/10.1016/j.apcatb.2015.01.014
0926-3373/

species [23,24]. The removal mechanisms of pollutants are known to be dependent on the surface property of the photocatalysts. For example, the mechanism of Cr(VI) photoreduction can be changed with the change of surface charge of g-C_3N_4 [25]. The adsorbed NO removal products can possibly change the surface property of photocatalysts because the incorporated formate anions can change the surface property of g-C_3N_4. Thus, the NO removal mechanism may be changed by the NO removal products. Moreover, the products of NO removal are dependent on the mechanisms of NO removal. The products of NO removal may also be changed with the change of NO removal mechanism. Meanwhile, understanding on NO removal mechanism help us modify photocatalysts for better NO removal activity.

Recently, bismuth oxyhalides (BiOX, X=Cl, Br, and I) as a novel ternary oxide semiconductor have drawn much attention because of their potential application in photocatalysis. Among them, BiOI is photochemically stable and has the smallest band gap (about 1.7–1.83 eV), which can be activated by visible light irradiation [26–28]. Moreover, study on the removal of air pollutants such as nitric oxide and its degradation mechanism using BiOI photocatalysts has not been reported. In this work, we selected the BiOI photocatalyst to investigate its photocatalytic properties in NO removal. We found that the NO removal product NO_3^- could change the NO removal process from nonselective oxidation to selective oxidation. A series of experiments was designed to investigate the products and mechanism of NO removal induced by BiOI. The reasons for the change of products and removal mechanism were also analyzed in detail. This is the first report on the photocatalytic degradation of NO using BiOI photocatalysts under visible light.

2. Experimental

2.1. Materials

The BiOI hollow spheres were synthesized using a solvothermal method. All the reagents were purchased from Sinopharm Chemical Reagent Co., Ltd. (Shanghai, China) without further purification. In a typical synthesis, 1.94 g of $Bi(NO_3)_3{\cdot}5H_2O$ (AR, 99.0%, 4 mmol) was dissolved in 70 mL of ethylene glycol. Potassium iodide (0.664 g; AR, 98.5%, 4 mmol) was then slowly added into the solution. The mixture was stirred for 0.5 h at room temperature in air and then transferred into a 100 mL Teflon-lined stainless autoclave. The autoclave was heated at 160 °C for 12 h under autogenous pressure and then air-cooled to room temperature. The resulting precipitates were collected and washed thoroughly with ethanol and deionized water several times, and then dried at 50 °C in air.

2.2. Characterization

Powder X-ray diffraction (XRD) patterns were recorded on a Rigaku D/MAX-RB diffractometer with monochromatized Cu Kα radiation (λ = 1.5418 Å). The morphologies were determined by scanning electron microscopy (SEM; JEOL 6700F). Transmission electron microscopy (TEM) images were obtained using a JEOL JSM-2010 microscope with an accelerating voltage of 200 kV. The samples for TEM were prepared by dispersing the final powders in ethanol, and then the dispersion was dropped on lacey support film grids. UV–vis diffuse reflectance spectra (DRS) were obtained using a UV–vis spectrometer (Shimadzu UV-3600) with $BaSO_4$ as a reference and were converted from reflection to absorbance by the Kubelka–Munk method. The FT-IR spectra of BiOI and used BiOI were collected using a Thermo Nicolet Nexus 670 spectrometer with a resolution of 4 cm^{-1}.

2.3. Photocatalytic activity test

The photocatalytic experiments of NO removal at ppb levels were performed at ambient temperature in a continuous flow reactor. The volume of the rectangular reactor, which was made of stainless steel and covered with quartz glass, was 4.5 L (30 cm × 15 cm × 10 cm [L × W × H]). One sample dish containing the BiOI film was placed in the middle of the reactor. An LED lamp (λ = 448 nm) was used as the visible light source. This lamp was vertically placed outside the reactor above the sample dish.

BiOI film was prepared by coating an aqueous suspension of BiOI onto a glass dish with a diameter of 12 cm. BiOI (0.15 g) was added into 15 mL of H_2O and ultrasonicated for 20 min. The aqueous suspension was then coated onto the glass dish, which was then dried at 60 °C until water was completely removed.

NO gas was obtained from a compressed gas cylinder at a concentration of 50 ppm NO (N_2 balance, BOC gas) with traceable National Institute of Standards and Technology specifications. The initial concentration of NO was diluted to about 600 ppb by the air stream supplied by a zero air generator. The gas streams were premixed by a gas blender, and the flow rate was controlled at 1 L/min by a mass flow controller. After adsorption–desorption equilibrium among gases and photocatalysts were achieved, the lamp was turned on. The concentration of NO was continuously measured using a chemiluminescence NO analyzer (Teledyne, NOx analyzer, model T200). The removal efficiency (η) of NO was calculated as follows:

$$5\eta(\%) = (1 - C/C_0) \times 100\%$$

where C and C_0 are the concentrations of NO in the outlet stream and feeding stream, respectively.

2.4. Trapping experiment

Potassium iodide (KI) is an effective hole scavenger, and tert-butyl alcohol (TBA) was selected as an •OH scavenger because it reacts with •OH radicals with a high rate constant ($k = 6 \times 10^8$). Potassium dichromate ($K_2Cr_2O_7$) was used to trap photogenerated electrons. Photocatalyst (0.15 g) with different trapping agents was added into 15 mL of H_2O and ultrasonicated for 20 min. The aqueous suspensions were then coated onto the glass dish. Subsequently, the coated dish was dried at 60 °C until water was completely removed. Finally, the coated dishes were used in NO removal experiments.

2.5. ESR measurement

All the ESR spectra were obtained with a Bruker EMX ESR Spectrometer (Billerica, MA) with employing 5,5-dimethyl-l-pyrroline-*N*-oxide (DMPO) as the spin trapper at room temperature. Fifty microliter aliquots of control or sample solutions were put in glass capillary tubes with internal diameters of 1 mm and sealed. The capillary tubes were inserted into the ESR cavity, and the spectra were recorded at selected times. Other settings were as follows: 1 G field modulation, 100 G scan range, and 20 m W microwave power.

3. Results and discussion

XRD was used to investigate the phase structures of the resulting samples. Fig. 1 shows the XRD pattern of the BiOI sample obtained from the solvothermal reaction. The BiOI sample was well crystallized and could be indexed to a pure hexagonal structure for BiOI (JCPDS file no. 73-2062). Fig. 2a and b show the SEM images of the BiOI sample. BiOI microspheres with sizes of about 1 μm to 3 μm were observed. Red circles indicate that the BiOI microspheres

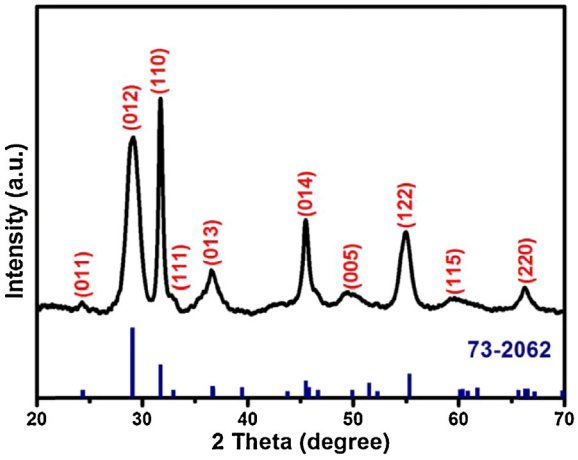

Fig. 1. The XRD pattern of the as-prepared BiOI sample.

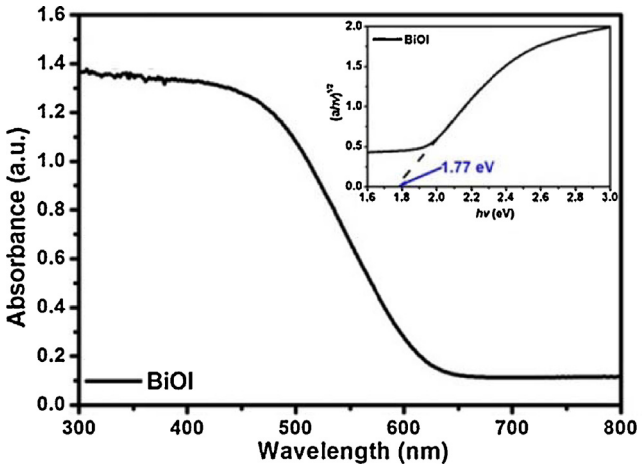

Fig. 3. The UV–vis absorption spectra and plots of $(\alpha h\nu)^{1/2}$ versus energy $(h\nu)$ of the as-prepared BiOI sample

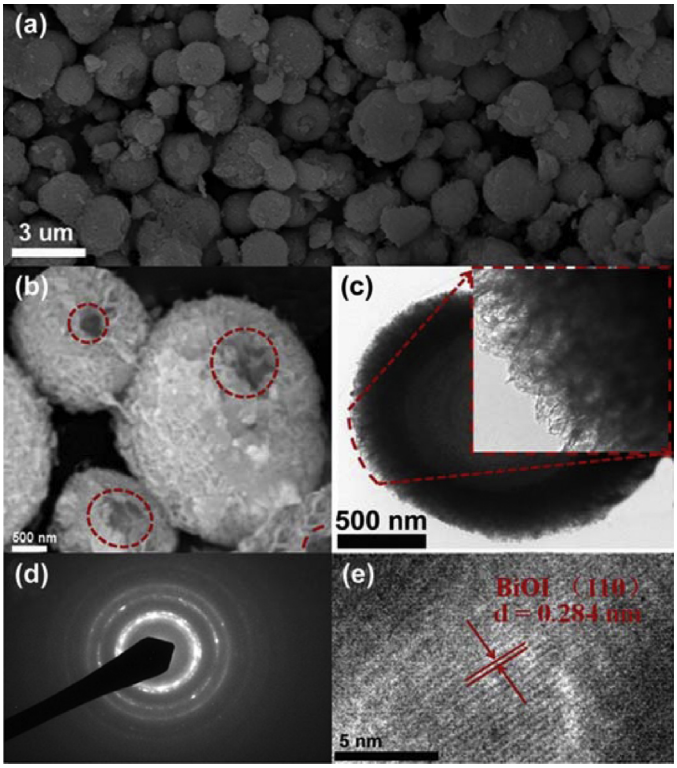

Fig. 2. (a), (b) SEM image of the as-prepared BiOI sample; (b) TEM images of the as-prepared BiOI sample; (c) the SAED pattern of the as-prepared BiOI sample; (d) the the high-resolution TEM image of the as-prepared BiOI sample.

were hollow and built by numerous interlaced 2D nanosheets. The morphology of BiOI was further characterized by TEM images that displayed the apparent microspheres (Fig. 2c). Irregular nanosheets were observed at the edge of the microsphere, which confirmed the nanosheet composition. The corresponding diffraction ring of the selected area electron diffraction (SAED) pattern identified the polycrystalline nature of BiOI hollow microspheres (Fig. 2d). Clear lattice fringes could be observed, and the lattice spacing matched the (0 1 2) plane of BiOI (Fig. 2e), which is in agreement with the results of XRD patterns shown in Fig. 1.

The UV–vis absorption spectrum of BiOI in Fig. 3a shows that BiOI possessed a good visible light absorption performance. Assuming that BiOI is an indirect semiconductor, plots of the $(ahV)^{1/2}$ versus the energy of absorbed light afford the band gaps of BiOI as shown in the inset of Fig. 3a. The calculated band gaps were approximately 1.77 eV for BiOI. This means that BiOI could be excited by the visible light before 700 nm.

The resulting BiOI was used to photocatalytically remove NO in air. Prior to visible light irradiation, the adsorption/desorption equilibrium between the gas and the BiOI was reached. The lamp was then turned on to initiate the photocatalytic removal of NO on the photocatalysts. Fig. 4a displays the NO concentration changes (C/Co) versus irradiation time in the presence of BiOI. NO could not be removed via direct photolysis under visible light irradiation without the presence of any photocatalysts. However, after we turned on the visible light, the NO concentration inside the reactor with BiOI sample started to decrease from around 600 ppb $(C/Co = 1)$ to around 240 ppb $(C/Co = 0.4)$ and reach a maximum removal percentage of around 60%. As the NO gas with initial concentration of around 600 ppb was continuously purged into the reactor throughout the whole process, it means that the photocatalyst can keep removing the 60% of NO under visible light when come out from the outlet of the reactor. The concentration change of NO followed the first-order kinetics, and the removal rate of NO over BiOI was 0.098 min^{-1}. In addition to NO concentration, we also monitored the concentration change of NO_2 in the NO removal process. After 40 min of visible light irradiation, a small amount of NO_2 was produced (Fig. 4b). This observation suggests that NO oxidation induced by BiOI is nonselective and that most NO was oxidized to NO_3^-. The existence of NO_3^- could be confirmed by FT-IR. The absorption band at 1623 cm^{-1} could be assigned to the stretching modes of BiOI (Fig. 5). The used BiOI exhibited a new band at 1384 cm^{-1}, which could be attributed to the stretching modes of NO_3^- groups.

To test the stability and practicality of BiOI for NO removal, we reused the catalyst for NO removal for four cycles under the same conditions, and the result is shown in Fig. 6. Fig. 6a reveals that the activity of BiOI did not decline after four cycles of NO photocatalytic removal under visible light irradiation, indicating that BiOI is stable and practical for NO photocatalytic removal. However, the amount of NO_2 generated after each cycle increased with increasing recycle number (Fig. 6b). The reaction from NO to NO_2 is a selective oxidation because NO_2 is a halfway oxidation product in NO removal process. We also analyzed the variation of NO_3^- concentration through FT-IR after each cycle. It can be seen from Fig. 7 that the amount of NO_3^- generated decreased with increasing recycle number (Noted that the concentration of NO_3^- displayed in FT-IR spectra are accumulation amount). Therefore, NO removal

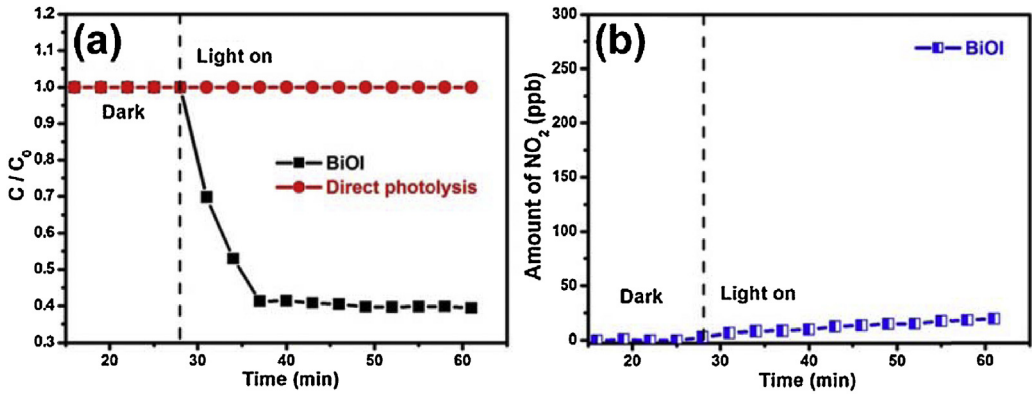

Fig. 4. (a) Comparison of the photocatalytic removal of NO in the presence and absence of BiOI sample; (b) the NO_2 generation over BiOI sample.

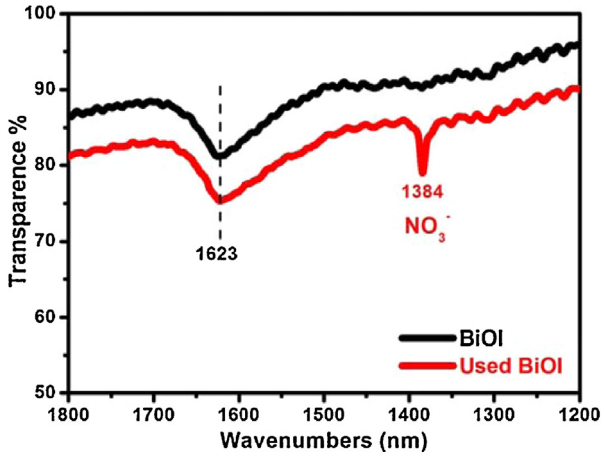

Fig. 5. The FTIR spectra of BiOI sample and used BiOI sample.

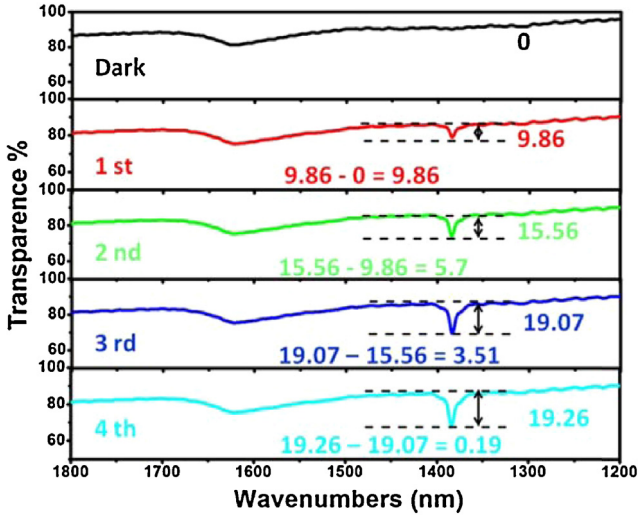

Fig. 7. The variation of the NO_3^- concentration with the increase of run cycle.

on the BiOI surface is a process that changes the oxidation from nonselective oxidation to selective oxidation.

Based on the change of NO removal production, two possible reasons were speculated for the change of NO removal from non-selective oxidation to selective oxidation. First, BiOI was gradually decomposed into a new photocatalyst, which has the same NO removal activity but has a different mechanism with BiOI. To test this possibility, we compared the XRD pattern of the original BiOI and the used BiOI (after four cycles). Significant change was not observed in the crystalline structure (Fig. 8); therefore, the first possible reason could be ruled out.

The second possible reason may be related to the generated NO_3^-. It adsorbed on the BiOI surface and may change the surface property and the NO removal mechanism of BiOI. Therefore, if NO_3^- is washed off from the BiOI surface, the NO removal production on the BiOI surface will be reverted from NO_2 to NO_3^-. To test this hypothesis, we collected the BiOI samples after four cycles and thoroughly washed with deionized water to remove the adsorbed NO_3^-. The washed BiOI was reused for NO removal for another four cycles. Fig. 9a shows that the activity of washed BiOI did not decline after another four cycles of NO photocatalytic removal under visible light irradiation, further indicating that the BiOI is stable and practical for NO photocatalytic removal. The amount of generated NO_2 in the

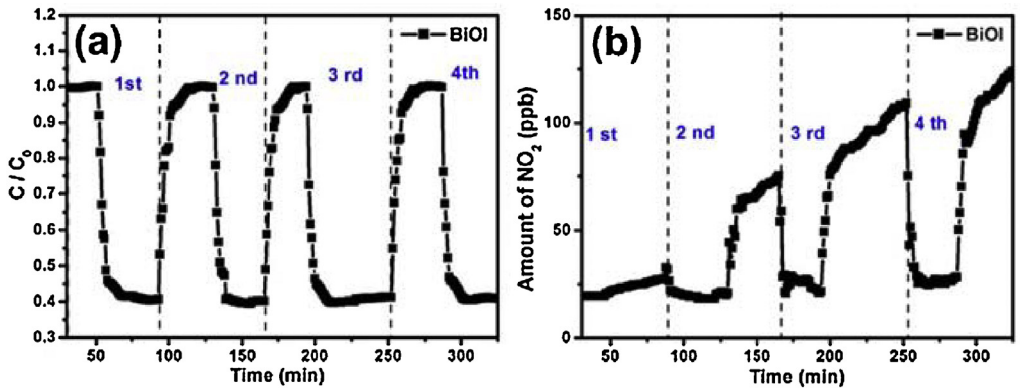

Fig. 6. (a) The stability of BiOI sample in multiple runs of NO removal; (b) the change of the NO_2 concentration with the increase of run cycles.

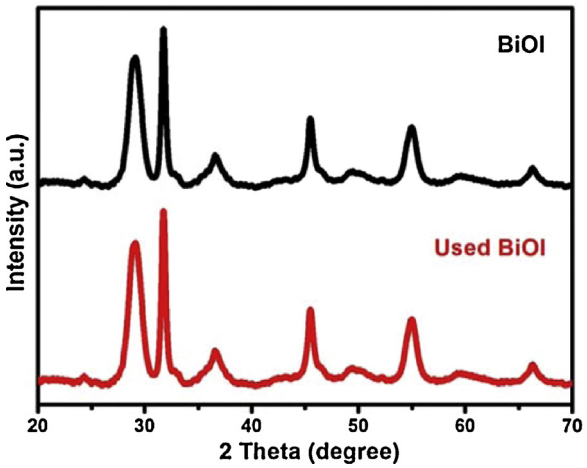

Fig. 8. The XRD patterns of BiOI and used BiOI samples.

fifth cycle was notably small (Fig. 9b). Because the NO removal process was reverted after the removal of surface NO_3^-, we conclude that the change process from nonselective oxidation to selective oxidation is related to the generated NO_3^-.

To further confirm that NO_3^- can change the NO removal process from nonselective oxidation to selective oxidation, we modified some NO_3^- on the surface of the original BiOI and used the resulting sample (NO_3^-–BiOI) as a photocatalyst to remove NO. Fig. 10 shows that the NO removal activity of NO_3^-–BiOI was similar to that of BiOI. However, the amounts of generated NO_2 over the two samples were different. In the BiOI system, a small amount of NO_2 was produced (19.8 ppb; Fig. 10a). By contrast, NO_2 was the main product in the NO_3^-–BiOI system under the same photocatalytic conditions and yielded 211.8 ppb (Fig. 10b). Obviously, the NO_3^- on the BiOI surface changed the NO removal process from nonselective oxidation to selective oxidation.

To determine the reasons for the change from nonselective oxidation to selective oxidation induced by NO_3^-, we conducted active species trapping experiments to investigate the possible photocatalytic removal mechanism of NO over BiOI. We carefully compared the trapping experiment results of BiOI (Fig. 11a). Adding $K_2Cr_2O_7$ slightly improved the NO removal activity of BiOI, suggesting that photogenerated electrons did not contribute to NO removal. However, KI and TBA could acutely depress the NO removal on BiOI, indicating that photogenerated holes and •OH are the main reactive species for the NO removal on BiOI. We measured the DMPO spin-trapping ESR spectra of BiOI in the aqueous dispersion for DMPO–OH (Fig. 11b). •OH could be generated in the BiOI system. Because electron trapping did not inhibit NO removal, we deduced that •OH could not be produced via an e^- $•O_2^-$ H_2O_2 •OH route. As the VB holes of BiOI can oxidize OH^- or H_2O into •OH because of their high potential energy, we therefore believe that •OH may be generated only via an h^+ OH^-/H_2O •OH route. Basing on the preceding experimental results and analysis, we proposed that the photogenerated holes contributed to the generation of •OH, and •OH may be responsible for the subsequent oxidation of NO.

$$BiOI + visiblelight \rightarrow h^+ + e^- \quad (1)$$

$$h^+ + OH^- \rightarrow •OH \quad (2)$$

$$•OH + NO \rightarrow NO_3^- \quad (3)$$

To clarify how the NO_3^- affects the mechanism of NO removal on the BiOI surface, active species trapping experiments were also carried out to investigate the possible photocatalytic removal mechanism of NO over NO_3^- BiOI (Fig. 11c). Adding TBA (10 mM, hydroxyl radical scavenger) or $K_2Cr_2O_7$ did not change the NO removal rate over NO_3^-–BiOI, suggesting that •OH and photogenerated electrons did not contribute to NO photoremoval. However,

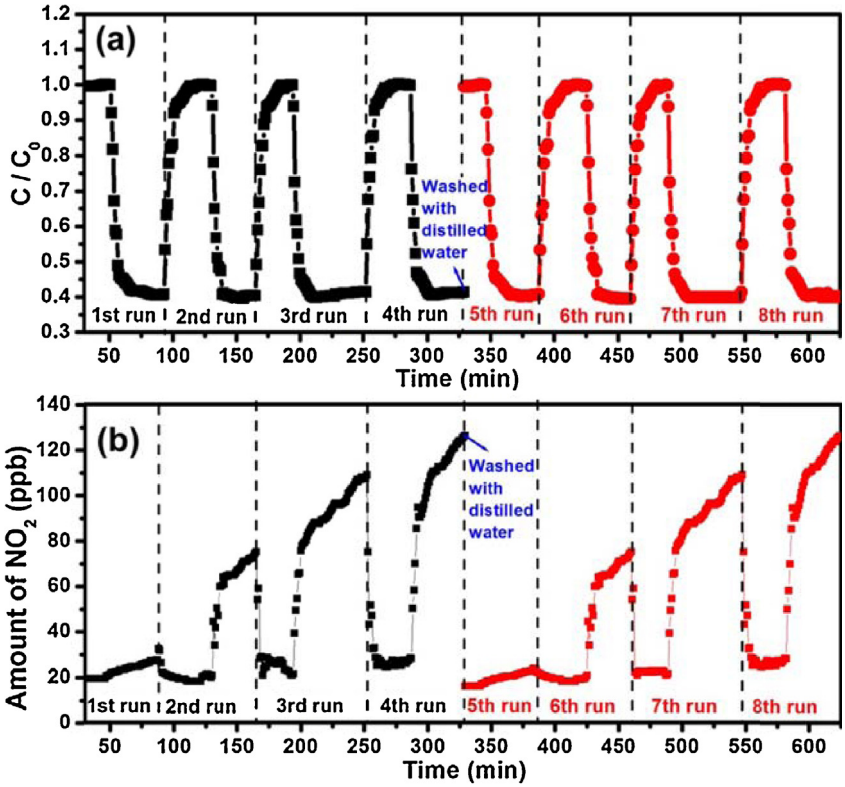

Fig. 9. (a) The stability of BiOI sample in multiple runs of NO removal (Samples were washed with distilled water after the fourth run); (b) the change of the NO_2 concentration with the increase of run cycles (Samples were washed with distilled water after the fourth run).

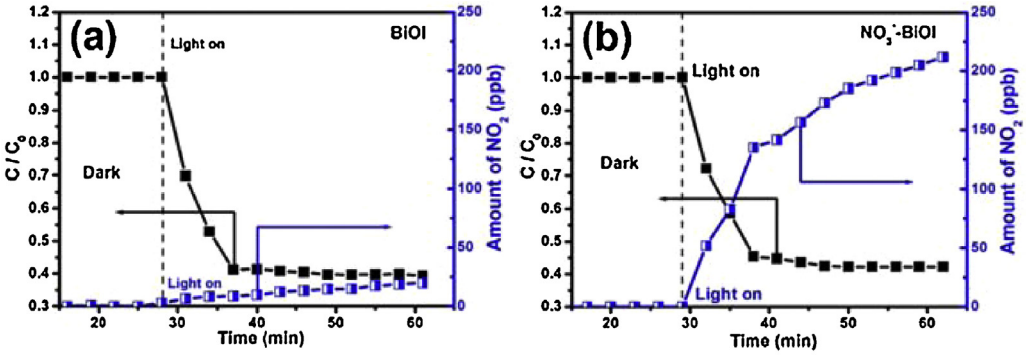

Fig. 10. (a) The photocatalytic removal of NO and the NO_2 generation in the presence of BiOI; (b) the photocatalytic removal of NO and the NO_2 generation in the presence of NO_3^-–BiOI.

KI (10 mM, hole scavenger) could acutely depress the NO removal on NO_3^-–BiOI, suggesting that photogenerated holes were the main reactive species for the NO removal on NO_3^-–BiOI. Photogenerated holes could directly oxidize NO to NO_2 because NO_2 was the main product of NO removal over NO_3^-–BiOI. This mechanism is quite different from that in the case of BiOI (Fig. 11a). We speculate that the surface of NO_3^- could inhibit the generation of •OH, and thus change the NO removal process from nonselective oxidation to selective oxidation. To confirm this conclusion, we also measured the DMPO spin-trapping ESR spectra of NO_3^-–BiOI in the aqueous dispersion for DMPO–OH (Fig. 11d). However, in contrast to BiOI, no peaks of •OH could be found in the aqueous dispersions of NO_3^--BiOI, confirming that the generated NO_3^- could inhibit •OH generation.

$$NO_3^-\text{–BiOI} + \text{visiblelight} \rightarrow h^+ + e^- \quad (4)$$

$$h^+ + NO \rightarrow NO_2 \quad (5)$$

Based on the preceding experiments, a possible photocatalytic removal pathway of NO in the BiOI system was proposed as follows (Fig. 12). First, hydroxyl ions were adsorbed on the surface active sites of BiOI. Hydroxyl ions would then be oxidized to •OH by the photogenerated holes. The subsequent reaction between •OH and NO produced NO_3^-, which would replace •OH

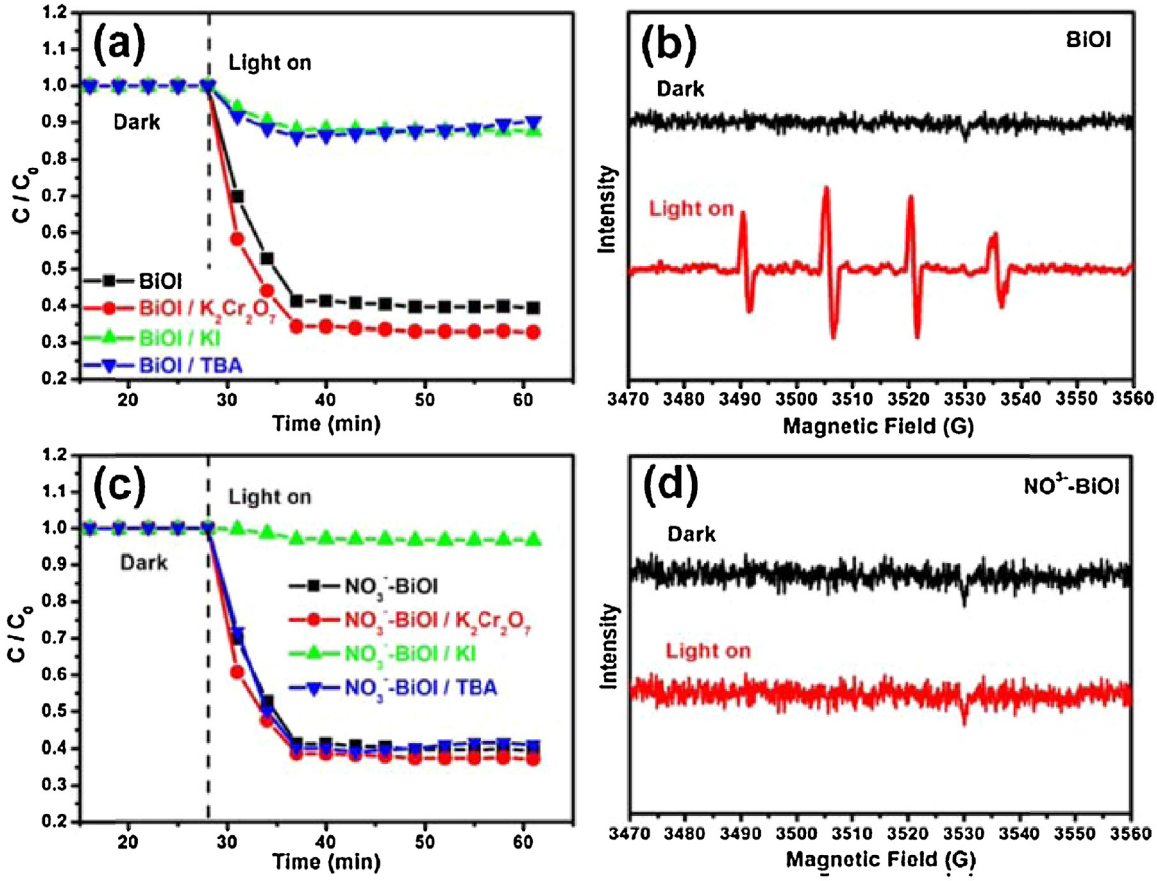

Fig. 11. (a) Comparison of photocatalytic activities of BiOI in different photocatalysis systems under visible light irradiation; (b) DMPO spin-trapping electron spin resonance spectra of BiOI suspension for DMPO–•OH; (c) Comparison of photocatalytic activities of NO_3^-–BiOI in different photocatalysis systems under visible light irradiation; (d) DMPO spin-trapping electron spin resonance spectra of NO_3^-–BiOI suspension for DMPO–•OH.

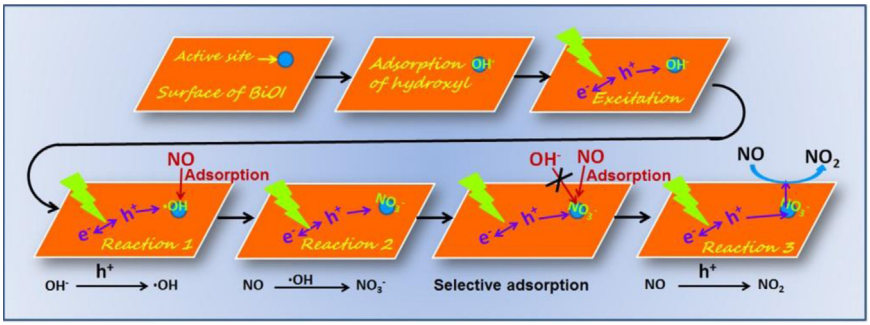

Fig. 12. The photocatalytic removal pathway of NO in the BiOI system.

to occupy the surface active sites of BiOI. Because like charges repel each other, hydroxyl ions would not be adsorbed again. In this case, •OH would not be produced. Therefore, NO was directly oxidized by photogenerated holes. Meanwhile, the products changed from NO_3^- to NO_2. The generated NO_3^- changed the NO removal process from nonselective oxidation to selective oxidation.

4. Conclusion

BiOI hollow microspheres were synthesized by the facile solvothermal method and used for the photocatalytic removal of NO under visible light irradiation. The process at the beginning of NO removal was nonselective oxidation because of the ultimate oxidation product at this stage (NO_3^-). As the irradiation time increased, nonselective oxidation gradually changed to selective oxidation because the product of NO removal changed from NO_3^- to NO_2. This change was related to the generated NO_3^-, which was produced from the reaction between NO and •OH. The generated NO_3^- could inhibit the generation of •OH and thus lead to the changes in the NO removal process. This study can improve our understanding on the NO removal mechanism and NO removal process on the photocatalyst surface and serve as a guide in using photocatalysts in NO removal.

Acknowledgements

This research is financially supported by the research grant of Early Career Scheme (ECS 809813) from the Research Grant Council, Hong Kong SAR Government, Dean's Research Fund-Early Career Researchers (04022), Research Equipment Grant (REG-2), and Internal Research Grant (R3429) from The Hong Kong Institute of Education.

References

[1] J.D. Felix, E.M. Elliott, S.L. Show, Environ. Sci. Technol. 46 (2012) 3528–3535.
[2] B. Rao, S. Mohan, A. Neuber, W.A. Jackson, Water Air Soil Pollut. 223 (2012) 275–287.
[3] J.A. Rodriguez, T. Jirsak, G. Liu, J. Hrbek, J. Dvorak, A. Maiti, J. Am. Chem. Soc. 123 (2001) 9597–9605.
[4] L.F. Wang, H. Chen, M.H. Yuan, S. Rivillon, E.H. Klingenberg, X.M. Li, R.T. Yang, Appl. Catal. B: Environ. 152–153 (2013) 162–167.
[5] N. Liu, Y.M. Xue, S. Hossain, N. Huang, D. Coursolle, J.A. Gralnick, E.M. Boon, Biochemistry 51 (2012) 2087–2099.
[6] J.C. Ball, M.D. Hurley, M.D. Hurley, A.M. Staccia, C.A. Gierzak, Environ. Sci. Technol. 33 (1999) 1175–1178.
[7] L.B. Kreuzer, L.K.N. Patel, Science 173 (1971) 45–47.
[8] B. Xiao, P.S. Wheatley, X.B. Zhao, A.J. Fletcher, S. Fox, A.G. Rossi, L.L. Megson, S. Bardiga, L. Regli, K.M. Thomas, R.E. Morris, J. Am. Chem. Soc. 129 (2007) 1203–1209.
[9] W.F. Yang, H.J. Hsing, Y.C. Yang, J.Y. Shyng, J. Hazard. Mater. 148 (2007) 653–659.
[10] S. BrÖer, T. Hammer, Appl. Catal. B: Environ. 28 (2000) 101–111.
[11] N.E. Khan, Y.G. Adewuyi, Ind. Eng. Chem. Res. 29 (2010) 8749–8760.
[12] Y.G. Adewuyi, N.Y. Sakyi, Ind. Eng. Chem. Res. 52 (2013) 11702–18760.
[13] G.S. Li, D.Q. Zhang, J.C. Yu, K.H. Leung, Environ. Sci. Technol. 44 (2010) 4276–4281.
[14] W.D. Zhang, Q. Zhang, F. Dong, Ind. Eng. Chem. Res. 52 (2013) 6740–6746.
[15] G.H. Dong, Z.H. Ai, L.Z. Zhang, RSC Adv. 4 (2014) 5553–5560.
[16] G.H. Dong, K. Zhao, L.Z. Zhang, Chem. Commun. 48 (2012) 6178–6180.
[17] Z.H. Ai, S.C. Li, Y. Huang, W.K. Ho, L.Z. Zhang, J. Hazard. Mater. 179 (2010) 141–150.
[18] N. Bowering, G.S. Walker, P.G. Harrison, Appl. Catal. B: Environ. 62 (2006) 208–216.
[19] Q.P. Wu, R.V.D. Krol, J. Am. Chem. Soc. 134 (2012) 9369–9375.
[20] J.Z. Ma, H.M. Wu, Y.C. Liu, H. He, J. Phys. Chem. C 118 (2014) 7434–7441.
[21] F. Dong, Z.Y. Wang, Y.H. Li, W.K. Ho, S.C. Li, Environ. Sci. Technol. 48 (2014) 10345–10353.
[22] Z.H. Ai, W.K. Ho, S.C. Li, L.Z. Zhang, Environ. Sci. Technol. 43 (2009) 4143–4150.
[23] J.C.S. Wu, Y.T. Cheng, J. Catal. 237 (2006) 393–404.
[24] Z.B. Wu, Z.Y. Sheng, Y. Liu, H.Q. Wang, N. Tang, J. Wang, J. Hazard. Mater. 164 (2009) 542–548.
[25] G.H. Dong, L.Z. Zhang, J. Phys. Chem. C 117 (2013) 4062–4068.
[26] L.Q. Ye, J.N. Chen, L.H. Tian, J.Y. Liu, T.Y. Peng, K.J. Deng, L. Zan, Appl. Catal. B: Environ. 130–131 (2013) 1–7.
[27] L.Q. Ye, L.H. Tian, T.Y. Peng, L. Zan, J. Mater. Chem. 21 (22) (2015) 12479–12484.
[28] M.Y. Ou, F. Dong, W. Zhang, Z.B. Wu, Chem. Eng. J. 255 (2014) 650–658.